

Catalytic action of two-dimensional layered materials (WS₂, and MoS₂) on hydrogen sorption properties of MgH₂

Satish Kumar Verma¹, Mohammad Abu Shaz¹, Thakur Prasad Yadav^{1,2}*

¹Hydrogen Energy Centre, Department of Physics, Banaras Hindu University, Varanasi-221005, India.

²Department of Physics, Faculty of Science, University of Allahabad, Prayagraj-211002, India.

Abstract:

The present study reports the catalytic action of two-dimensional (2D) layered materials (MoS₂ and WS₂) for improving the de/re-hydrogenation kinetics of MgH₂. The MgH₂ start desorbing at 277 °C with a hydrogen storage capacity of 5.95 wt% in the presence of WS₂ catalyst whereas onset desorption temperature of MgH₂ catalyzed by MoS₂ is 330 °C. The MgH₂-WS₂ absorbed hydrogen ~ 3.72 wt% within 1.3 minutes at 300 °C under 13 atm hydrogen pressure and it desorbed ~5.57 wt% within 20 minutes at 300 °C under 1 atm hydrogen pressure. We have performed 25 cycles of dehydrogenation (under 1 atm hydrogen pressure at 300 °C) and re-hydrogenation (under 13 atm hydrogen pressure at 300 °C) to ensure cyclic stability of catalyzed version of MgH₂ where MgH₂-WS₂ shows better cyclic stability than MgH₂-MoS₂. MgH₂-WS₂ also shows the lower reaction activation energy ~117 kJ/mol as compare to other catalyzed and uncatalyzed samples. On the other hand, these catalysts (WS₂ and MoS₂) do not have any impact on the thermodynamical parameters that is change in enthalpy.

Key words: 2D layered materials, De/re-hydrogenation kinetics, Activation energy, MgH₂.

*Corresponding author Email: yadavtp@gmail.com

1. Introduction

A crucial and promising area of research for onboard hydrogen applications is the development of safe and efficient hydrogen storage. The solid-state approach is one of the most appropriate, secure, and effective ways to store hydrogen among the several methods that can be used, including gaseous, liquid, and solid-state storage [1,2]. Due to its high hydrogen storage capacity (110 g/L volumetric and 7.6 wt% gravimetric), low cost, light weight, and large abundance (in the form of Mg) in earth crust (8th most) and seawater (3rd most), MgH₂ is a leading choice for hydrogen storage in the solid-state mode [3–6]. According to the United States Department of Energy (US DOE) technical targets for hydrogen storage systems [7], MgH₂ has certain advantages that make it a viable option. The high dehydrogenation temperature (above 400 °C), slow kinetics (hydrogen de/re-hydrogenation kinetics 0.4 kg-H₂/min), and high thermodynamic properties (high reaction enthalpy 74 kJ/mol) of MgH₂ prevent it from being a suitable material for onboard applications even with these advantages [8–10]. In recent years, the creation of suitable catalyst(s), alloys, composite materials with complicated hydrides, and scaffolding have all been used as feasible methods to improve the hydrogen storage performance of MgH₂ [11,12]. The use of various types of catalysts and additives to enhance the performance of Mg/MgH₂ has been the subject of several studies by various research organizations [13–17].

Another application for the 2D materials is as a catalyst for improving the hydrogen characteristics of MgH₂ [18–22]. Due to its enormous surface area, ballistic conduction, thermal conductivity, mechanical stability, and light weight, graphene, which has a 2D planer structure with sp² carbon atoms arranged in a hexagonal framework, has attracted a lot of attention as a catalyst and as a template material for hydrogen storage application in MgH₂ [23,24]. MgH₂'s de/rehydrogenation kinetics exhibit effective catalytic behavior in the graphene layer, which also inhibits MgH₂'s agglomeration and grain growth [3,5,25]. Liu et al., for instance, have created MgH₂-5% Gr nanosheets [26]. They have demonstrated that graphene nanosheets offer a significant hydrogen diffusion pathway and prevent MgH₂ from aggregating. According to Huang et al., [27] report's MgH₂ nanoparticles supported by graphene exhibit remarkable hydrogen sorption kinetics and

cyclic stability. Due to the strong interaction between graphene and MgH₂ nanoparticles and the prevention of nanoparticle agglomeration, the MgH₂ nanoparticles demonstrated excellent hydrogen storage performance. Additionally, graphene prevents the aggregation of nanoparticles during the rehydrogenation of MgH₂, according to a theoretical study using molecular dynamics simulation [28]. Rough studies are still required to determine the impact of graphene and other 2D layered materials on MgH₂, even though some prior studies have shown the remarkable catalytic/co-catalytic and agglomeration blocking properties of Gr on MgH₂.

We have examined a comparison between WS₂ and MoS₂ as a catalyst for enhancing hydrogen sorption properties of MgH₂. WS₂ and MoS₂ are suitable alternatives to graphene for the catalytic action on MgH₂ due to their high conductivity (metallic nature), thermal stability, and strong catalytic behavior [29,30]. Tungsten (W) and Molybdenum (Mo) are sandwiched between two Sulphur layers with weak Van der Waals interactions in the family of layered transition-metal dichalcogenides (TMDs) materials that include WS₂ and MoS₂. The re/de-hydrogenation kinetics, and catalytic behavior of WS₂ and MoS₂ on MgH₂ has been investigated in details.

2. Experimental section

2.1. Synthesis of a few layered WS₂

The bulk tungsten sulfide (WS₂) (99.80 %) powder was procured from the Alfa Aesar for the present investigation. For the preparation of few layered WS₂, WS₂ powder was dispersed in de-ionized water and sonicated it for 74 hours using ultrasonicator at 20 kHz frequency. The sonicated sample was then dried at 50 °C under a dynamic vacuum of order 10⁻² torr to form the few layered WS₂ powder. This preparation method can also be understood by the schematic given in Fig. 1.

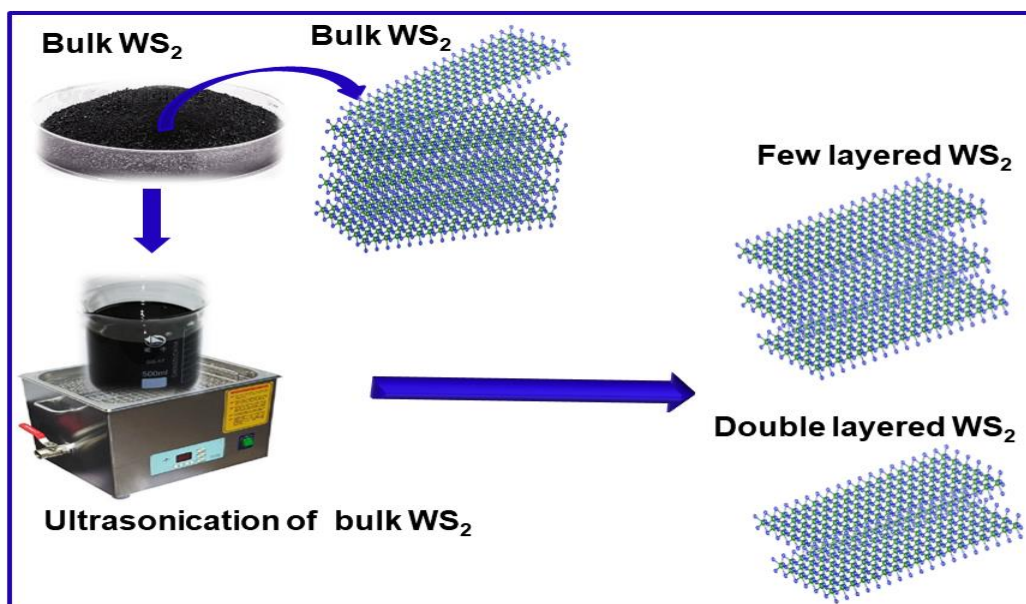


Fig.1: Schematic diagram for the synthesis of a few layers WS₂.

2.2. Synthesis of few-layer MoS₂

The Otto Chemica bulk molybdenum disulfide (MoS₂) (99 %) powder was used for the present investigation. MoS₂ powder was dispersed in de-ionized water and sonicate it for 74 hours using ultrasonicator at 20 kHz frequency to obtain the few-layered MoS₂. The sonicated sample was then dried at 50 °C under dynamic vacuum of order 10⁻² torr to form the few layered MoS₂ powder. Fig. 2, shows the schematic diagram for preparation of few-layered MoS₂.

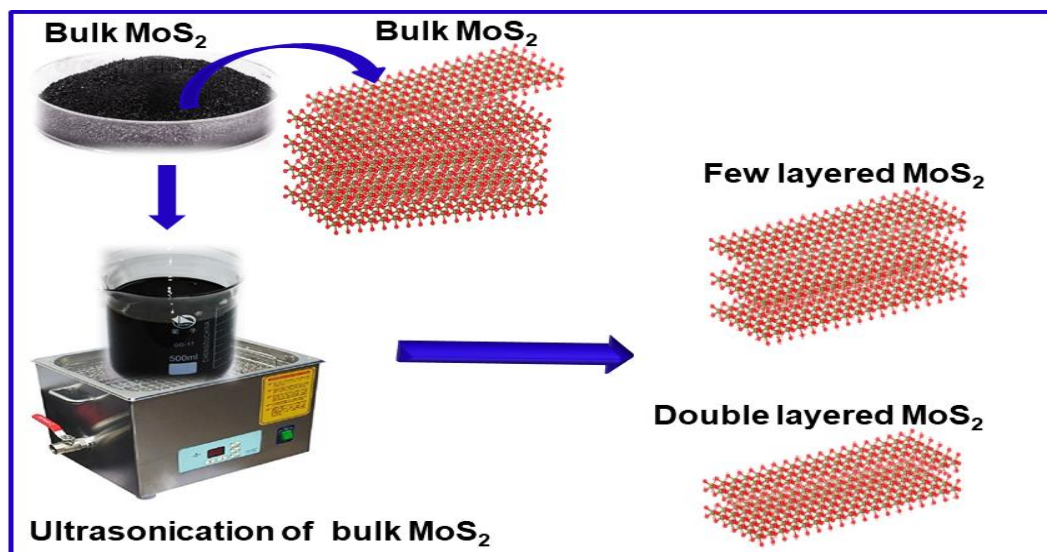


Fig.2: Schematic diagram for the synthesis of a few layers MoS₂.

2.3. Synthesis of MgH₂ catalyzed by WS₂, and MoS₂

The pure MgH₂ was procured from Fujifilm (Japan) (99.9%) for the present investigation. Mechanical ball-milling of MgH₂ with graphene at 180 rpm for 24 hours with a ball-to-powder ratio of 50:1 (by weight) using a planetary ball-miller (Retsch PM 400) was used to synthesize MgH₂ catalyzed by WS₂ (MgH₂-WS₂). To explore the optimum catalyst concentration for hydrogen sorption kinetics of Mg/MgH₂, we have synthesized a set of different catalyst concentrations (5, 10, 12 wt%) to catalyze MgH₂. For hydrogen sorption in Mg/MgH₂, 10 wt% catalysts were found to be optimal (in terms of desorption temperature and hydrogen storage capacity). The ball-miller vials were filled with 5 atm H₂ pressure to compensate for the loss of hydrogen from MgH₂ during milling. All the loading and unloading of the samples was done inside the N₂-filled glove box (MBRAUM MB10 compact) with O₂ and H₂O levels < 1 ppm. The synthesis of MgH₂ catalyzed by MoS₂ (MgH₂-MoS₂) was done using the same synthesis route as MgH₂-WS₂.

2.4. Characterization techniques

The structural characterization of prepared samples was carried out by XRD technique using Empyrean PANalytical X-ray diffractometer equipped with 2D detector with a Cu K α beam ($\lambda = 1.5415 \text{ \AA}$) operated at 40 kV and 40 mA. The microstructural and selected area electron diffraction (SAED) analysis of as-prepared samples was carried out by TEM (Technai-20G²) operating at the accelerating voltage of 200 kV. Perkin Elmer (Spectrum 100) spectrometer in transmission mode with attenuated total reflectance (ATR) sampling mode (wavenumber range 500–4000 cm⁻¹) was used to carry out FTIR spectroscopy. The Raman spectra have been acquired at -60 °C using Horiba-Jobin-Yvon LABRAM-HR800 spectrometer with diode LASER (532 nm). The desired thickness and surface topography of the prepared samples were examined by using solver next AFM in non-contact mode. The characterized samples then proceed for the hydrogen desorption and absorption using automated two-channel volumetric sieverts type apparatus. The temperature programmed desorption (TPD) was carried out with a heating rate of 5 °C-

min⁻¹. The activation energy (E_a) study of prepared catalyzed samples has been done by using DSC (Perkin Elmer DSC 8000) with a heating rate of 15 °C/min, 18 °C/min, 21 °C/min, and 24 °C/min under nitrogen atmosphere (20 ml/min).

3. Results and discussion

3.1. Structural, microstructural, and spectroscopic characterization analysis

The structural characteristics of as-prepared samples have been examined using the XRD characterization. Fig. 3(a) shows the XRD pattern of pristine MgH₂, which matches well with the tetragonal MgH₂ with space group P42/mnm (136) and $a=b= 4.516 \text{ \AA}$, $c = 3.020 \text{ \AA}$ (JCPDS no. 740934). Fig. 3(b) shows the XRD pattern of MoS₂, which matches well with the hexagonal structure of MoS₂ with space group P63/mmc(194) and $a=b= 3.1602 \text{ \AA}$, $c = 12.294 \text{ \AA}$ (Joint Committee on Powder Diffraction Standards (JCPDS) no. 651951). The XRD pattern of as-prepared WS₂ is shown in Fig. 3(c), that matches well with the hexagonal structure of WS₂ with space group P63/mmc(194) and $a=b= 3.1532 \text{ \AA}$, $c = 12.323 \text{ \AA}$ (JCPDS no. 841398). The usual diffraction pattern of MgH₂-MoS₂, and MgH₂-WS₂ are shown in Fig. 3(d-e), respectively, where besides the tetragonal phase of MgH₂, some peaks of WS₂ and MoS₂ are either suppressed or masked by the peaks of MgH₂. The diffraction peaks of WS₂ and MoS₂ are identified and labeled in the Fig. 3(d-e), respectively.

The different bands position, shapes, and relative intensities of Raman spectra give us essential information about the materials and stacking of layers, i.e., Raman spectroscopy can determine the layer thickness at the atomic level. The Raman spectra of as-prepared WS₂, and MoS₂ have shown in Fig. 4. In the case of MoS₂, the two Raman modes are appeared at $\sim 345 \text{ cm}^{-1}$ and $\sim 370 \text{ cm}^{-1}$ corresponds to E_{2g}^1 and A_{1g} modes of vibrations (labeled in Fig. 4(b)). The indicated modes of MoS₂ have frequency difference of $\sim 25 \text{ cm}^{-1}$, that means the MoS₂ as layered material with few layers of stacking (3-5 layers) [31,32]. The FWHM of A_{1g} mode is $\sim 7 \text{ cm}^{-1}$, which can also be referred to stacking a few layers of MoS₂ [33]. The Raman shifts at $\sim 316 \text{ cm}^{-1}$ and 384 cm^{-1} (shown in Fig. 4(a)) corresponds to the presence of E_{2g}^1 and A_{1g} modes respectively in WS₂ sample. The

intensity ratio of E^{1}_{2g} and A_{1g} modes was estimated E^{1}_{2g}/A_{1g} i.e. = 1.26, which is higher than the intensity ratio of bulk WS_2 ($E^{1}_{2g}/A_{1g} = 0.47$) and lower than the monolayer WS_2 ($E^{1}_{2g}/A_{1g} = 2.2$) [34,35]. This calculated intensity ratio ($E^{1}_{2g}/A_{1g} = 1.26$) is compatible with the range of 2-3 layers of WS_2 .

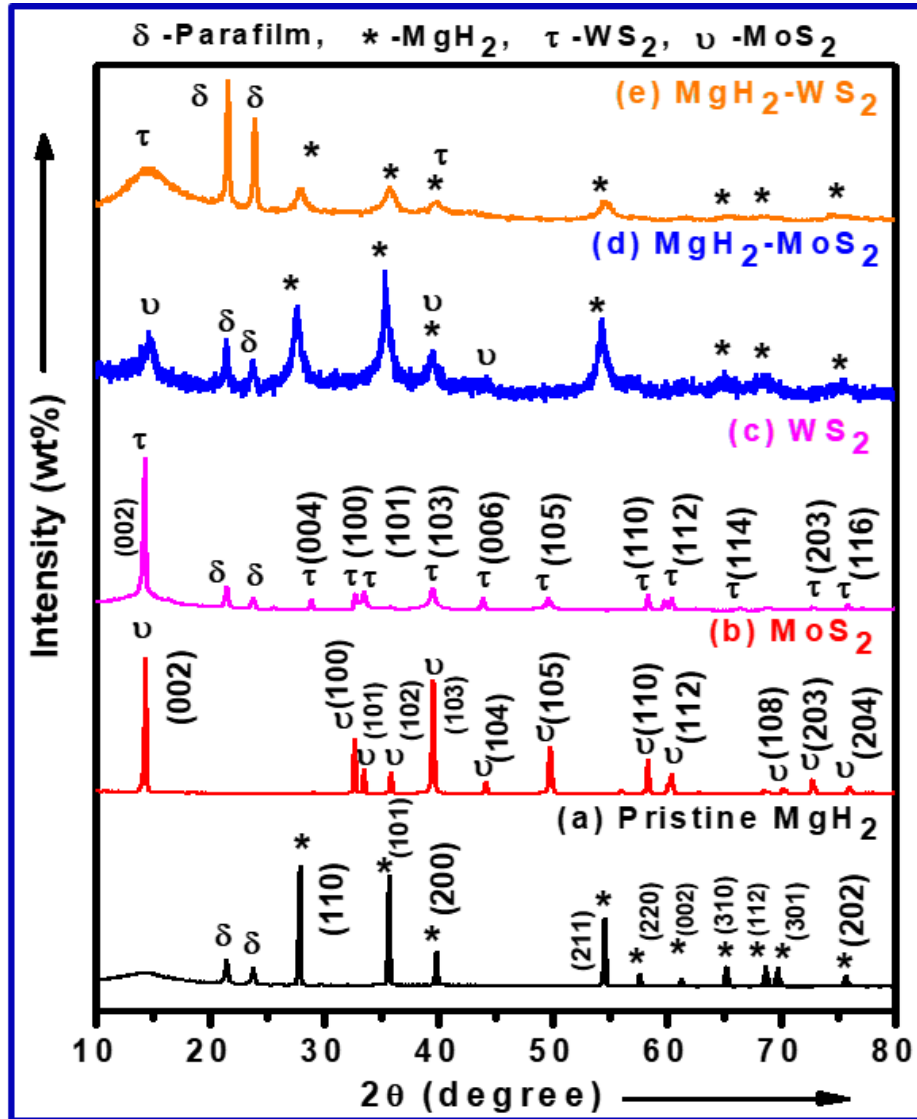


Fig. 3: XRD patterns of (a) Pristine MgH_2 , (b) MoS_2 , (c) WS_2 , (d) MgH_2-MoS_2 , and (e) MgH_2-WS_2 .

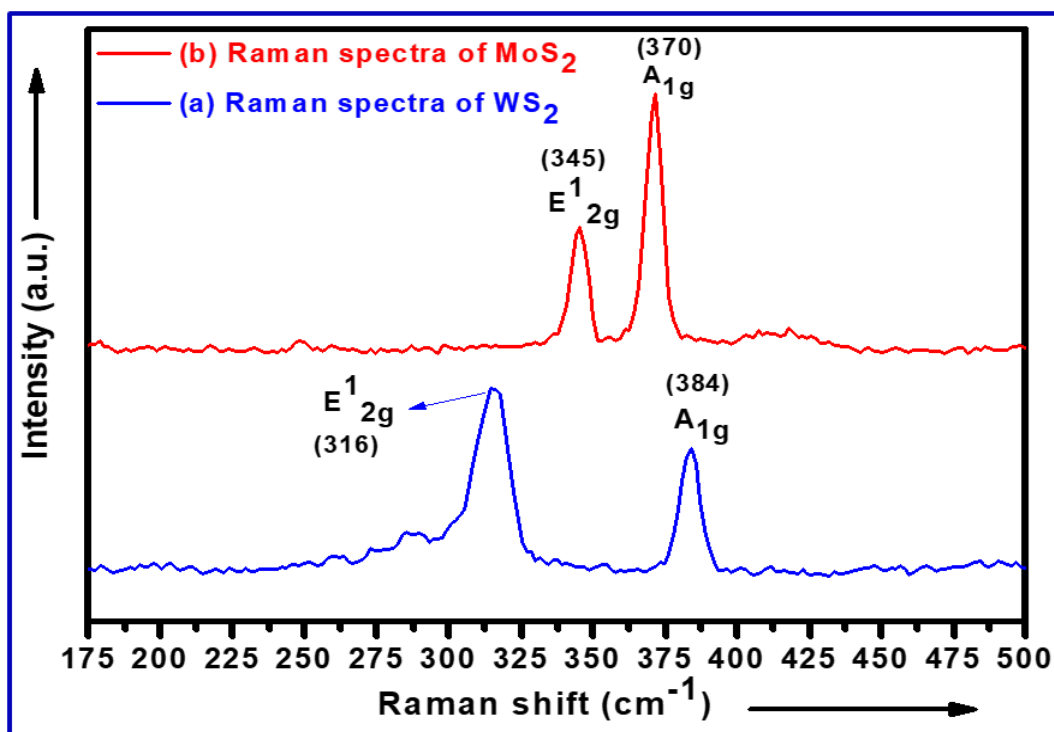


Fig. 4: Raman spectra of (a) WS₂ and (b) MoS₂.

The information about stacking layers in 2D layered materials (like WS₂ and MoS₂) can also be verified by AFM analysis. The surface topography and height profile of prepared MoS₂, and WS₂ were examined along the blue dotted line as shown in Fig. S1(a-b) (given in supporting information). The layered surface morphology along with height profile (shown in Fig. S1(a-a1)) shown the average thickness of MoS₂ is ~1.3 nm, that indicates the presence of ~2 layers of stacking in the MoS₂ sample [36,37]. The ~7-8 layers of stacking were present in the case of WS₂ (shown in Fig. S1(b-b1)) with a monolayer height of ~0.7 nm [38].

3.2 De/Re-hydrogenation kinetics of catalyzed MgH₂

To identify the optimal percentage of catalyst in MgH₂ with optimum temperature range where material performed promptly, we have characterized as-prepared samples for the temperature programmed desorption (TPD) analysis. The TPD curves of MgH₂-MoS₂ have seen in Fig. S2 (given in supporting information). The MgH₂-5%MoS₂, MgH₂-10%MoS₂, and MgH₂-12%MoS₂, starts releasing hydrogen at ~ 357 °C, ~ 330 °C, ~ 302 °C with ~ 6.41 wt%, ~ 6.00 wt%, ~ 4.88 wt% of hydrogen storage capacity respectively. On the other hand, MgH₂-5%WS₂, MgH₂-10%WS₂, and MgH₂-12%WS₂, starts releasing hydrogen at ~ 339 °C, ~ 277 °C, ~ 258 °C with ~ 6.54 wt%, ~ 5.95 wt%, ~ 5.14 wt% of hydrogen storage capacity respectively (shown in Fig. S3 in supporting information). Based on TPD analysis, the optimum catalyst concentration for catalyzing MgH₂ is 10 wt% for all catalysts.

After getting information about the optimum catalyst for MgH₂, we compared the TPD analysis of all optimum catalyzed samples with pristine MgH₂, as shown in Fig. 5. The TPD of pristine MgH₂ (shown in Fig. 5(a)) was then carried out to compare hydrogen storage properties with catalyzed samples. The pristine MgH₂ has an onset desorption temperature of 376 °C with a total release of ~7.45 wt% storage capacity. The onset desorption temperature of MgH₂-MoS₂ (MgH₂-10%MoS₂) is ~ 330 °C, and it desorbs ~ 6.00 wt% hydrogen while the desorption gets completed at 396 °C (Fig. 5(b)). In the case of MgH₂-WS₂ (MgH₂-10%WS₂), it starts desorbing hydrogen at ~ 277 °C with a storage capacity of 5.95 wt% (Fig. 5(c)).

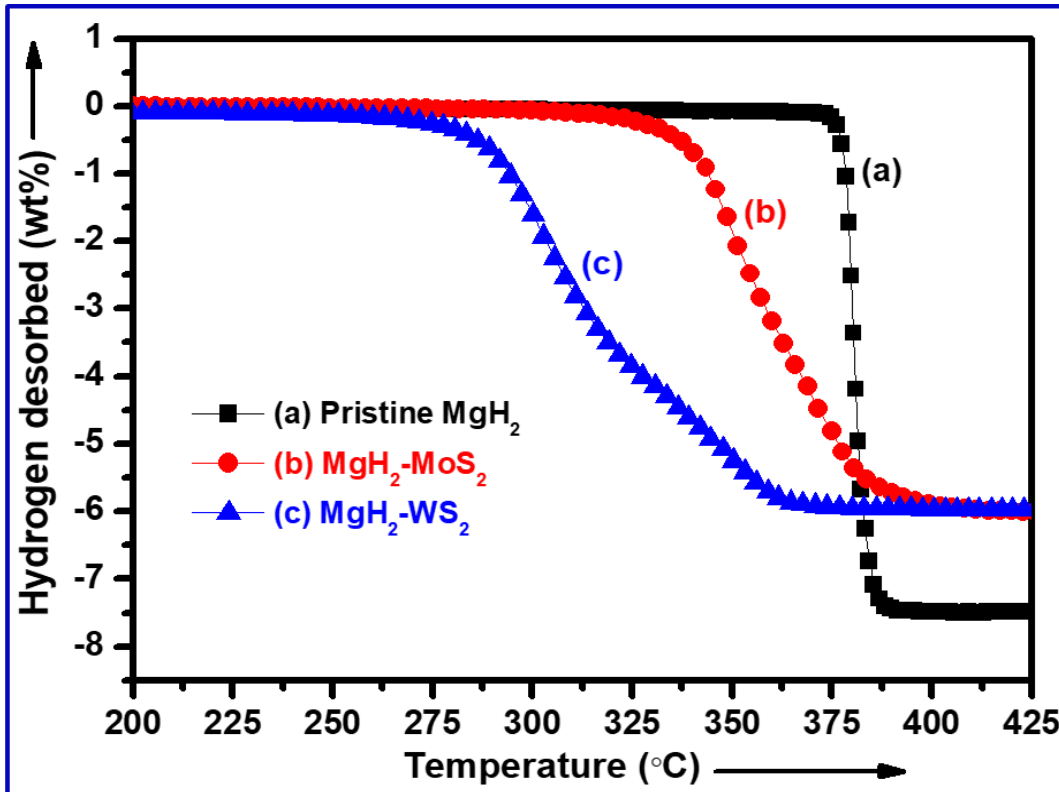


Fig. 5: Comparative TPD analysis of (a) Pristine MgH₂, (b) MgH₂-MoS₂ and (c) MgH₂-WS₂.

The desorbed samples then proceed for re/de-hydrogenation to check the cyclic stability and reversibility of catalyzed and pristine MgH₂. The re-hydrogenation kinetics was carried out at 300 °C under 13 atm hydrogen pressures, as shown in Fig. 6. It can be seen, the pristine MgH₂ absorbed ~1.16 wt% hydrogen in 1.2 minutes whereas MgH₂-MoS₂, MgH₂-WS₂ absorbed 4.60 wt%, 3.72 wt%, hydrogen, respectively, under similar conditions of temperature and pressure.

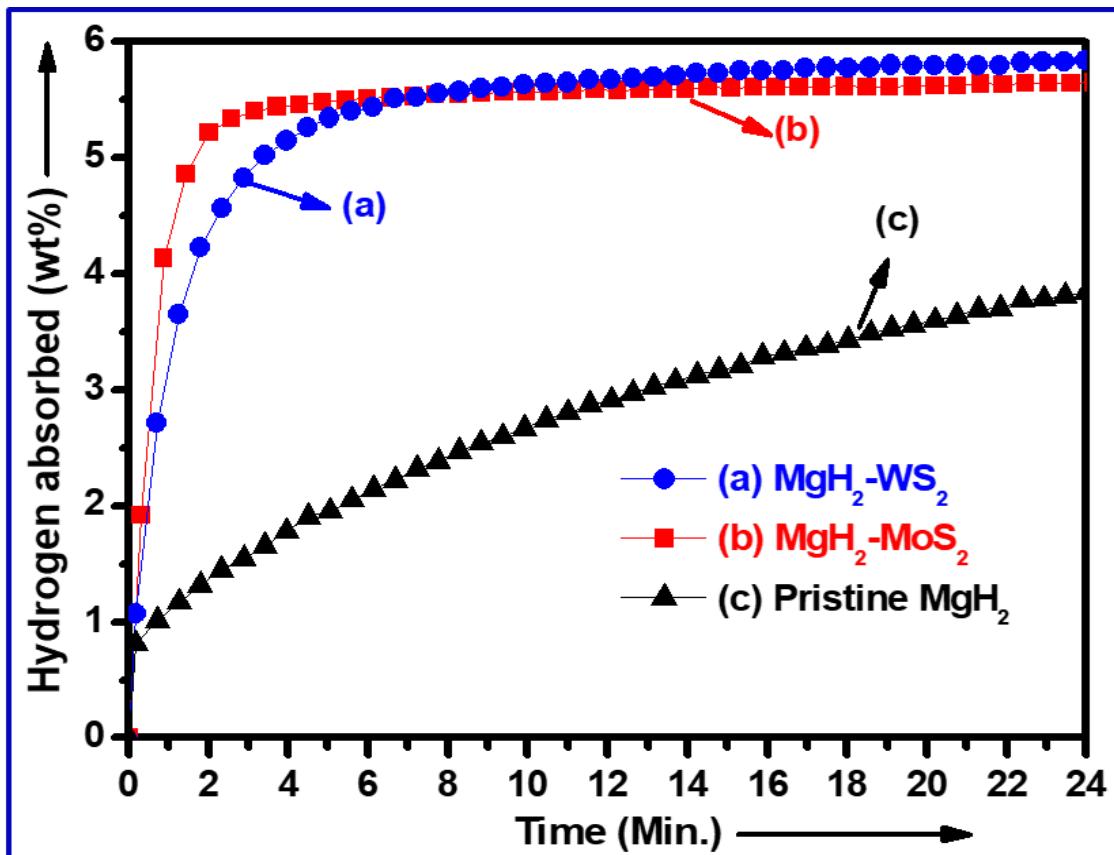


Fig. 6: Rehydrogenation kinetics curves at 300 °C under 13 atm H₂ pressure of (a) b) MgH₂-WS₂, (c) MgH₂-MoS₂ and (e) Pristine MgH₂.

The rehydrogenated samples were then dehydrogenated at 300 °C under 1 atm hydrogen pressure. It can be seen clearly in Fig. 7, that the MgH₂-WS₂ sample releases 5.57 wt% hydrogen within 20 minutes while MgH₂-MoS₂ and pristine MgH₂ releases 2.25 wt%, and 0.23 wt% of hydrogen under similar temperature and pressure conditions, which is 3.32 wt%, and 4.48 wt% more than pristine MgH₂, MgH₂-MoS₂, respectively. Based on the above re/de-hydrogenation kinetics study, it is clearly shown that WS₂ works as a superior catalyst to MoS₂ for catalyzing MgH₂. Therefore, in present study WS₂ is a prominent catalyst to catalyze MgH₂.

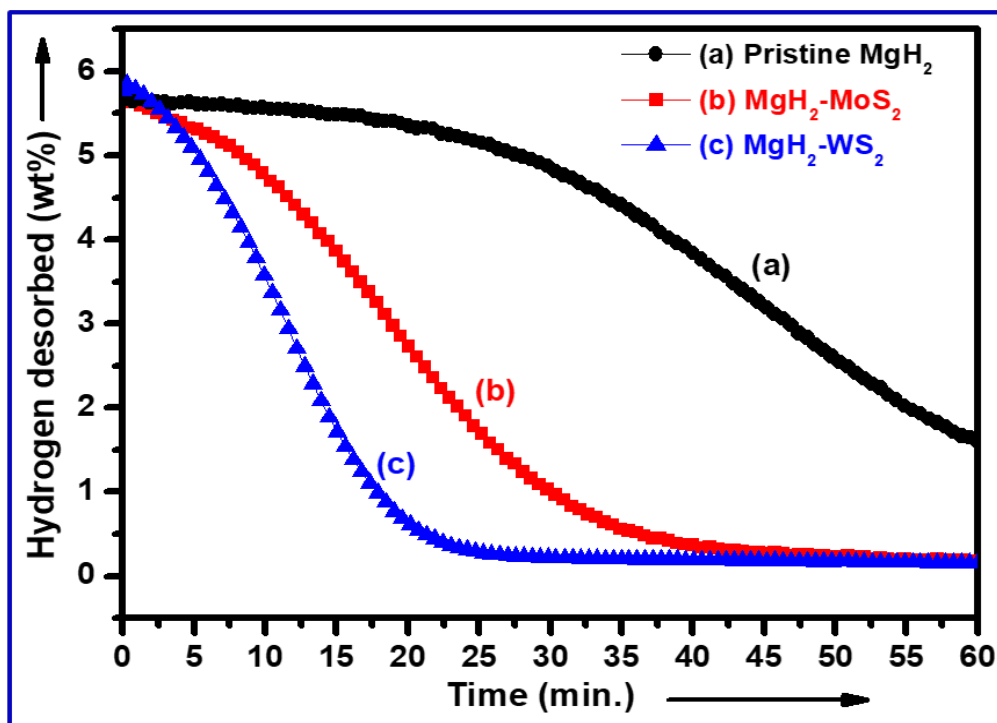


Fig. 7: Dehydrogenation kinetics curves at 300 °C under 1 atm H₂ pressure of (a) MgH₂-WS₂, (b) MgH₂-MoS₂, and (c) Pristine MgH₂.

3.3. Study of kinetics: Estimation of activation energy

The DSC was carried out to determine the hydrogen desorption activation energy barrier to convert MgH₂ into Mg. The DSC profile of MgH₂-MoS₂, MgH₂-WS₂, are shown in Figs. 8-9. In the case of MgH₂-WS₂, the peak desorption temperature found from DSC is ~ 380 °C, while the onset desorption temperature found from TPD is ~ 277 °C. There is a difference in desorption temperature in TPD (Fig. 5(c)) and DSC (Fig. 9(a)) curves due to the TPD being performed under vacuum with a temperature ramping rate of 5 °C/min while DSC was performed under N₂ atmosphere with a temperature ramping rate of 15 °C/min. For calculating the desorption activation energy, we have performed DSC with a set of the various rate of heating (15, 18, 21, 24 °C/min) and plotted the Kissinger curve by using the Kissinger equation[39] as given:

$$\ln(\beta/T_p^2) = \left(-\frac{E_a}{RT_p}\right) + \ln(k_o) \quad (1)$$

Where β , T_p , and E_a are the heating rate, corresponding peak desorption temperature, and activation energy, respectively. The slope of Kissinger plot ($\ln(\beta/T_p^2)$ vs. $1000/T_p^2$ plot) (Figs. 8-9) is used to calculate the desorption activation energy. The calculated activation energy for MgH₂-MoS₂, and MgH₂-WS₂ is 117.09 kJ/mol (± 1.60 kJ/mol), and 104.00 kJ/mol (± 2.74 kJ/mol) respectively. This activation energy indicates that ~104 kJ/mol energy is required to overcome the barrier to convert MgH₂ into Mg in the presence of a WS₂ catalyst. These calculated activation energies are significantly lower than the activation energy of pristine MgH₂ [3,40].

Table 1: Table for plateau pressures at corresponding temperatures, change in enthalpy, and activation energy of MgH₂-MoS₂, and MgH₂-WS₂.

S.No.	Sample name	Plateaus pressure (atm)	Temperature (°C)	Change in enthalpy (kJ/mol)	Activation energy (kJ/mol)
1.	MgH ₂ -MoS ₂	1.03	272.62	-78.33	117.09
		2.03	292.28		
		3.77	313.28		
2.	MgH ₂ -WS ₂	1.52	281.26	-77.44	104.66
		2.92	300.60		
		3.45	316.29		

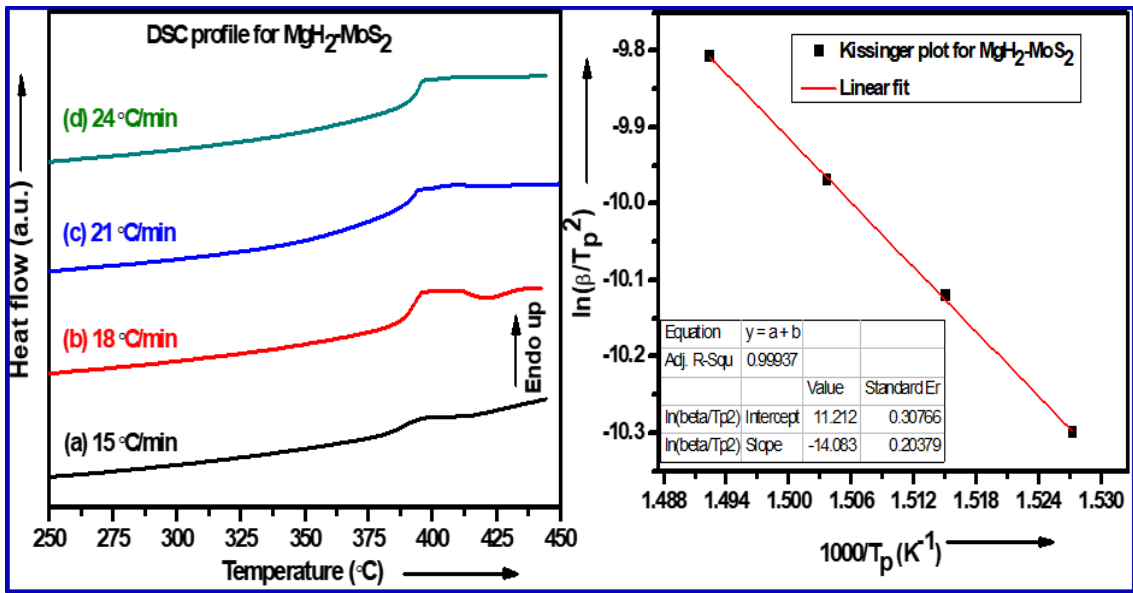


Fig. 8: (i) DSC profile for desorption of $\text{MgH}_2\text{-MoS}_2$ with the heating rate (a) 15 $^{\circ}\text{C}/\text{min}$, (b) 18 $^{\circ}\text{C}/\text{min}$, (c) 21 $^{\circ}\text{C}/\text{min}$, (d) 24 $^{\circ}\text{C}/\text{min}$, and (ii) corresponding Kissinger plot for evaluating the desorption activation energy of $\text{MgH}_2\text{-MoS}_2$.

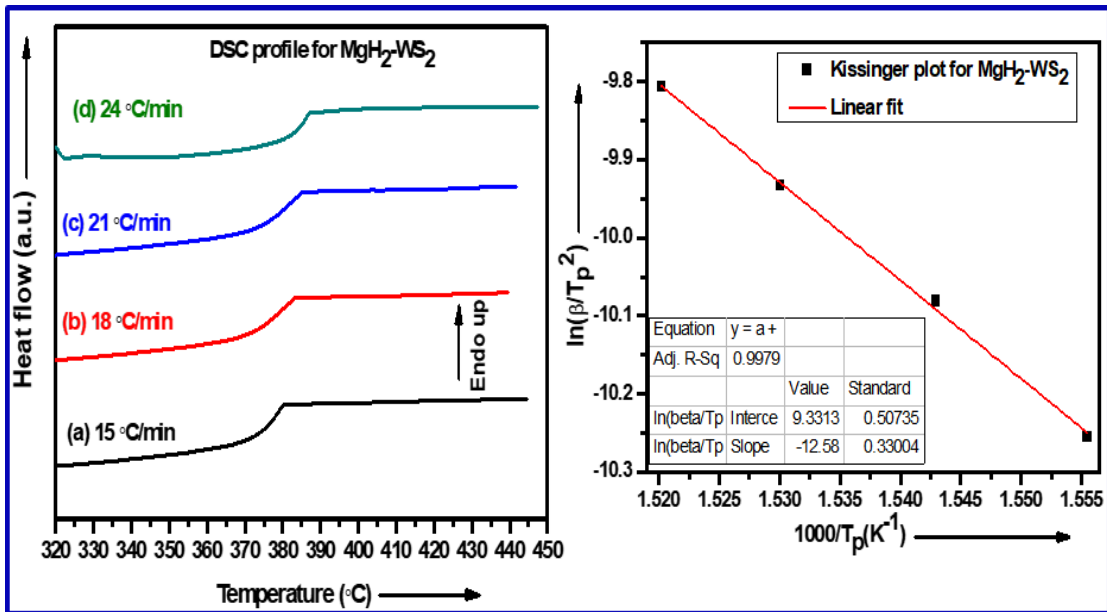


Fig. 9: (i) DSC profile for desorption of MgH₂-WS₂ with the heating rate (a) 15 °C/min, (b) 18 °C/min, (c) 21 °C/min, (d) 24 °C/min, and (ii) corresponding Kissinger plot for evaluating the desorption activation energy of MgH₂-WS₂.

3.4. Study of thermodynamics

After the kinetics and reversibility study, we have proceeded with the thermodynamic analysis of catalyzed MgH₂ for comparing the change in enthalpy and entropy of the system using well known Van't Hoff equation [41].

$$\ln P = (\Delta H/RT) - (\Delta S/R) \quad (2)$$

Where P, ΔH, R, T, and ΔS are the pressure, change in enthalpy, gas constant, absolute temperature, and change in entropy, respectively. The PCI isotherms (Figs. 10(i)-11(i)) and Van't Hoff plots (Figs. 10(ii)-11(ii)) were used for the calculation of change in enthalpy of MgH₂-MoS₂ and MgH₂-WS₂, respectively. The calculated change in desorption enthalpy was found to be 78.33 kJ/mol (± 1.40 kJ/mol), and 77.44 kJ/mol (± 1.13 kJ/mol), for MgH₂-MoS₂ and MgH₂-WS₂ respectively. It is clear from the above estimation of change in enthalpy, that there is no significant enthalpy change in the presence of a catalyst. Thus MoS₂, WS₂ have not positively impacted the thermodynamic barrier of the MgH₂. The plateau pressure at corresponding temperatures, change in enthalpy, and activation energy has been tabulated in Table 1.

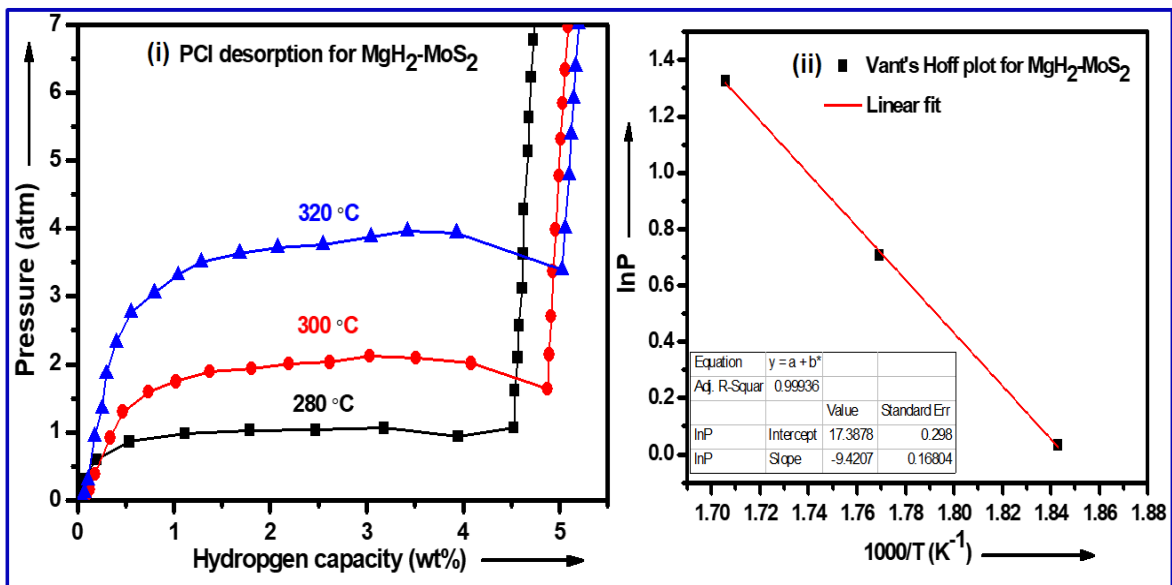


Fig. 10: (i) PCI desorption plots for MgH₂-MoS₂ at different temperatures and (ii) corresponding Van't Hoff plot for calculating the change in enthalpy

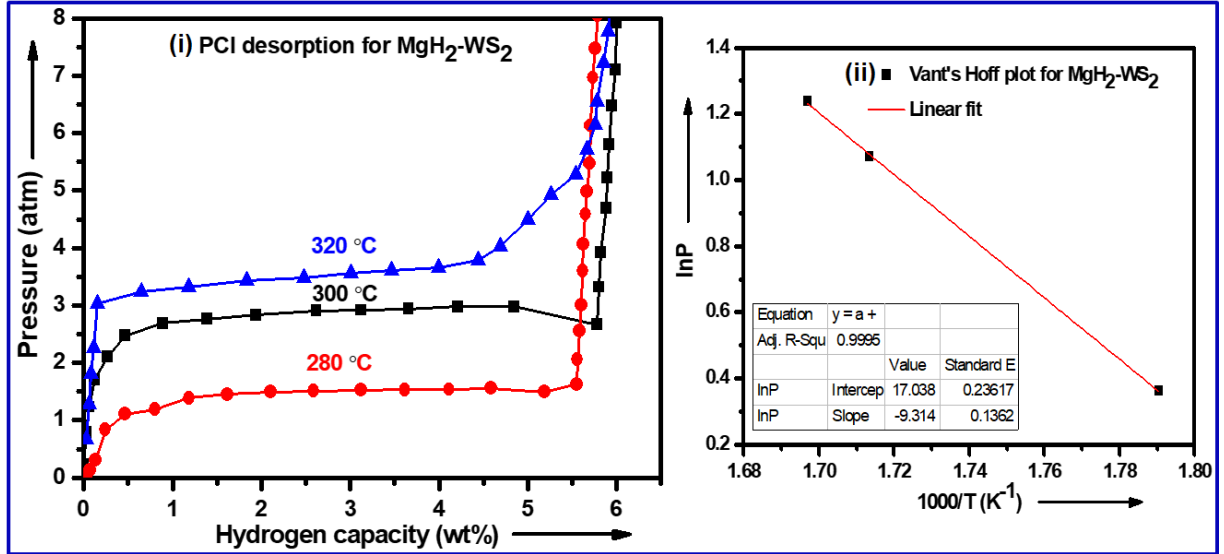


Fig. 11: (i) PCI desorption plots for MgH₂-WS₂ at different temperatures and (ii) corresponding Van't Hoff plot for calculating the change in enthalpy

3.5 Cyclic stability of catalyzed MgH₂

The WS₂ (optimum catalyst) plays a significant role in improving the kinetics of MgH₂. The cyclic stability is an essential characteristic of the hydride material (MgH₂) besides kinetic and thermodynamics, making it a worthy hydrogen storage material. Therefore, it is crucial to look at the cyclic stability of the catalyzed MgH₂ samples. We have performed 25 cycles of dehydrogenation (under 1 atm hydrogen pressure at 300 °C) and re-hydrogenation (under 13 atm hydrogen pressure at 300 °C) to ensure cyclic stability of catalyzed MgH₂. The cyclic stability curve of MgH₂-MoS₂ and MgH₂-WS₂ are shown in Fig. 12. From Fig. 12(a) MgH₂-MoS₂ shows the ~ 0.42 wt% (from 5.77 wt% to 5.35 wt%) degradation in hydrogen storage capacity during rehydrogenation and ~ 0.38 wt% (from 5.69 wt% to 5.31 wt%) in dehydrogenation. The MgH₂-WS₂ has the loss of hydrogen storage capacity ~ 0.3 wt% (from 5.80 wt% to 5.50 wt%) during rehydrogenation and ~ 0.36 wt% (from 5.76 wt% to 5.40 wt%) during dehydrogenation. Thus, MgH₂-WS₂ has more substantial cyclic stability than MgH₂-MoS₂ under similar

temperature and pressure conditions. The comparative study for hydrogen storage properties of different recently used 2D materials as the catalyst for MgH_2 is explored in Table 2.

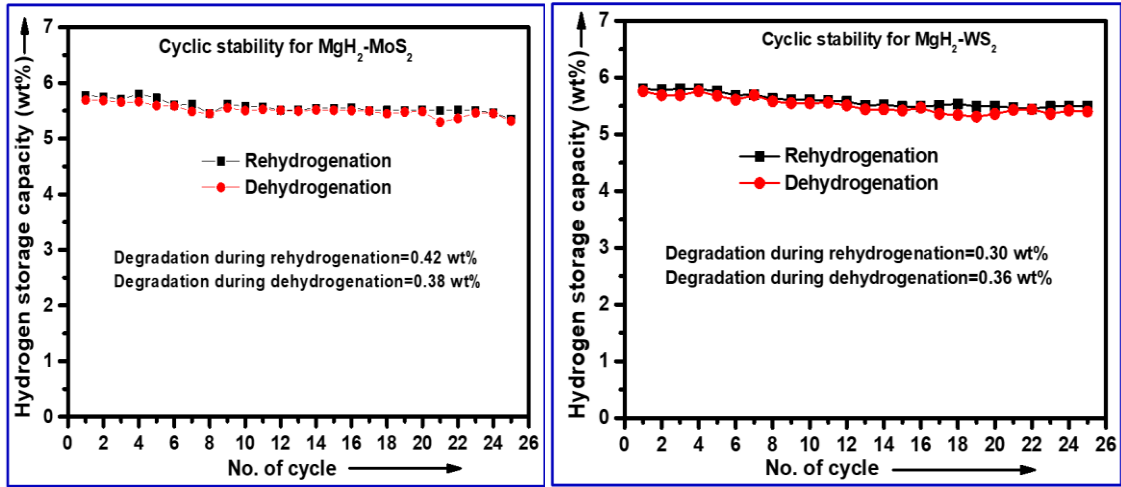


Fig. 12: Cyclic stability of (a) MgH_2 - MoS_2 and (b) MgH_2 - WS_2 .

Table 2: Table for different 2D materials as the catalyst for hydrogen storage application.

S. No.	Material	2D- based catalyst	Hydrogen storage capacity (wt%)	Onset dehydrogenation temperature (°C)	Activation energy (kJ/mol)	Change in enthalpy (kJ/mol)	Ref.
1.	Mg_6C_2N	C_2N	6.79	--	--	--	[20]
2.	MgH_2 - $LiAlH_4$ - Ti_3C_2	Ti_3C_2	6.50	63.0	128.4	74.3	[22]
3.	MgH_2 - $Nb_4C_3T_x$	$Nb_4C_3T_x$	3.50	150.6	81.2	--	[21]
4.	1T'- MoS_2		3.90	--	--	--	[42]
5.	MgH_2 -Gr	Graphene	5.80	300.0	--	--	[43]

6.	MgH ₂ -TiH ₂ @Gr	Graphene	6.77	204.0	88.89	74.54	[3]
	MgH ₂ -TiO ₂ @Gr	Graphene	5.98	240.0	98.00	76.87	
	MgH ₂ -Ti@Gr	Graphene	5.70	235.0	103.03	75.65	
7.	MgH ₂ -Gr	Graphene	6.14	300.0	134.95	77.90	[13]
8.	MgH ₂ -VS ₂	VS ₂	6.51	242.0	98.10	76.83	
9.	MgH ₂ -WS ₂	WS ₂	5.95	277.0	104.66	77.44	Present study
10.	MgH ₂ -MoS ₂	MoS ₂	6.00	330.0	117.09	78.33	Present study

4. Conclusions

The catalytic effect of MoS₂, and WS₂ on MgH₂ was evaluated and compared. Based on the de/re-hydrogenation study, it is found that WS₂ works as an optimum catalyst over MoS₂ for MgH₂. The MgH₂-WS₂ has an onset de-hydrogenation ~277 °C with a hydrogen storage capacity of 5.95 wt%. The MgH₂-WS₂ absorbed hydrogen ~ 3.72 wt% within 1.3 minutes at 300 °C under 13 atm hydrogen pressure and it desorbed ~5.57 wt% within 20 minutes at 300 °C under 1 atm hydrogen pressure. The MgH₂-WS₂ shows a minimum degradation of hydrogen storage capacity ~ 0.3 wt% upto 25 cycles which shows a better cyclic stability than cyclic stability of MgH₂-MoS₂ (~ 0.4 wt% loss in hydrogen storage capacity). MgH₂-WS₂ also shows the lower reaction activation energy ~117 kJ/mol as compare to other catalyzed and uncatalyzed samples. On the other hand, these catalysts (WS₂ and MoS₂) do not have any impact on the thermodynamical parameters that is change in enthalpy. This study opens a new era to further applications of 2D layered materials for various applications like template materials.

Acknowledgments

We gratefully accept funding assistance from the Department of Science and Technology (DST), New Delhi, India. The Council of Scientific and Industrial Research (CSIR), New Delhi, India, has awarded the author (S.K.V.) a CSIR-Senior Research Fellowship (Award No. 09/013(0872)/2019-EMR-I), for which the author is grateful.

Conflict of Interest Declaration

There are no conflicts of interest among the authors.

References

- [1] TP Yadav, A Kumar, SK Verma, NK Mukhopadhyay, High-Entropy Alloys for Solid Hydrogen Storage: Potentials and Prospects, *Transactions of the Indian National Academy of Engineering*, 7 (2022) 147–156.
<https://doi.org/10.1007/s41403-021-00316-w>.
- [2] A. Kumar, T.P. Yadav, N. K. Mukhopadhyay, Notable hydrogen storage in Ti–Zr–V–Cr–Ni high entropy alloy, *International Journal of Hydrogen Energy* 47 (2022) 22893–22900. <https://doi.org/10.1016/j.ijhydene.2022.05.107>
- [3] Verma SK, Bhatnagar A, Shukla V, Soni PK, Pandey AP, Yadav TP, et al. Multiple improvements of hydrogen sorption and their mechanism for MgH₂ catalyzed through TiH₂@Gr. *Int J Hydrogen Energy* 2020;45:19516–30.
<https://doi.org/10.1016/j.ijhydene.2020.05.031>.
- [4] SK Pandey, SK Verma, A Bhatnagar, TP Yadav, Catalytic characteristics of titanium-(IV)-isopropoxide (TTIP) on de/re-hydrogenation of wet ball-milled MgH₂/Mg, *International Journal of Energy Research* 46 (12) (2022) 17602–17615.
<https://doi.org/10.1002/er.8427>.
- [5] Shukla V, Bhatnagar A, Verma SK, Pandey AP, Vishwakarma AK, Srivastava P, et al. Simultaneous improvement of kinetics and thermodynamics based on SrF₂ and SrF₂@Gr additives on hydrogen sorption in MgH₂. *Mater Adv* 2021;2:4277–90. <https://doi.org/10.1039/D1MA00012H>.
- [6] Srivastava ON, Yadav TP, Shahi RR, Pandey SK, Shaz MA, Bhatnagar A.

- Hydrogen energy in India: Storage to application. Proc Indian Natl Sci Acad 2015;81:915–37. <https://doi.org/10.16943/ptinsa/2015/v81i4/48303>.
- [7] US DoE. Target Explanation Document: Onboard Hydrogen Storage for Light-Duty Fuel Cell Vehicles. US Drive 2017:1–29.
- [8] Bhatnagar A, Pandey SK, Vishwakarma AK, Singh S, Shukla V, Soni PK, et al. Fe₃O₄ @graphene as a superior catalyst for hydrogen de/absorption from/in MgH₂ /Mg. J Mater Chem A 2016;4:14761–72. <https://doi.org/10.1039/c6ta05998h>.
- [9] Sadhasivam T, Kim H-T, Jung S, Roh S-H, Park J-H, Jung H-Y. Dimensional effects of nanostructured Mg/MgH₂ for hydrogen storage applications: A review. Renew Sustain Energy Rev 2017;72:523–34. <https://doi.org/https://doi.org/10.1016/j.rser.2017.01.107>.
- [10] Yartys VA, Lototskyy M V, Akiba E, Albert R, Antonov VE, Ares JR, et al. Magnesium based materials for hydrogen based energy storage: Past, present and future. Int J Hydrogen Energy 2019;44:7809–59. <https://doi.org/https://doi.org/10.1016/j.ijhydene.2018.12.212>.
- [11] SK Pandey, A Bhatnagar, SS Mishra, TP Yadav, MA Shaz, ON Srivastava, Curious Catalytic Characteristics of Al–Cu–Fe Quasicrystal for e/Rehydrogenation of MgH₂, The Journal of Physical Chemistry C 121 (45) (2017) 24936-24944. <https://doi.org/10.1021/acs.jpcc.7b07336>
- [12] V Shukla, TP Yadav, Notable catalytic activity of CuO nanoparticles derived from metal-organic frameworks for improving the hydrogen sorption properties of MgH₂, International Journal of Energy Research, 46 (9) (2022) 12804-12819. <https://doi.org/10.1002/er.8050>.
- [13] Verma SK, Shaz MA, Yadav TP. Enhanced hydrogen absorption and desorption properties of MgH₂ with graphene and vanadium disulfide. Int J Hydrogen Energy 2022. <https://doi.org/https://doi.org/10.1016/j.ijhydene.2021.12.269>.
- [14] Patelli N, Calizzi M, Migliori A, Morandi V, Pasquini L. Hydrogen Desorption Below 150 °C in MgH₂–TiH₂ Composite Nanoparticles: Equilibrium and Kinetic Properties. J Phys Chem C 2017;121:11166–77. <https://doi.org/10.1021/acs.jpcc.7b03169>.
- [15] Korablov D, Besenbacher F, Jensen TR. Kinetics and thermodynamics of

- hydrogenation-dehydrogenation for Mg-25% TM (TM = Ti, Nb or V) composites synthesized by reactive ball milling in hydrogen. *Int J Hydrogen Energy* 2018;43:16804–14. <https://doi.org/10.1016/j.ijhydene.2018.05.091>.
- [16] Bhatnagar A, Johnson JK, Shaz MA, Srivastava ON. TiH₂ as a Dynamic Additive for Improving the De/Rehydrogenation Properties of MgH₂: A Combined Experimental and Theoretical Mechanistic Investigation. *J Phys Chem C* 2018;122:21248–61. <https://doi.org/10.1021/acs.jpcc.8b07640>.
- [17] Zhang J, Xia G, Guo Z, Zhou D. Synergetic Effects toward Catalysis and Confinement of Magnesium Hydride on Modified Graphene: A First-Principles Study. *J Phys Chem C* 2017;121:18401–11. <https://doi.org/10.1021/acs.jpcc.7b05848>.
- [18] Singh MK, Bhatnagar A, Pandey SK, Mishra PC, Srivastava ON. Experimental and first principle studies on hydrogen desorption behavior of graphene nanofibre catalyzed MgH₂. *Int J Hydrogen Energy* 2017;42:960–8. <https://doi.org/10.1016/J.IJHYDENE.2016.09.210>.
- [19] Liu G, Wang Y, Jiao L, Yuan H. Understanding the role of few-layer graphene nanosheets in enhancing the hydrogen sorption kinetics of magnesium hydride. *ACS Appl Mater Interfaces* 2014;6:11038–46. <https://doi.org/10.1021/am502755s>.
- [20] Varunaa R, Ravindran P. Potential hydrogen storage materials from metal decorated 2D-C₂N: An: ab initio study. *Phys Chem Chem Phys* 2019;21:25311–22. <https://doi.org/10.1039/c9cp05105h>.
- [21] Liu Y, Gao H, Zhu Y, Li S, Zhang J, Li L. Excellent catalytic activity of a two-dimensional Nb₄C₃T_x (MXene) on hydrogen storage of MgH₂. *Appl Surf Sci* 2019;493:431–40. <https://doi.org/https://doi.org/10.1016/j.apsusc.2019.07.037>.
- [22] Chen G, Zhang Y, Cheng H, Zhu Y, Li L, Lin H. Effects of two-dimension MXene Ti₃C₂ on hydrogen storage performances of MgH₂-LiAlH₄ composite. *Chem Phys* 2019;522:178–87. <https://doi.org/https://doi.org/10.1016/j.chemphys.2019.03.001>.
- [23] Raccichini R, Varzi A, Passerini S, Scrosati B. The role of graphene for electrochemical energy storage. *Nat Mater* 2015;14:271–9. <https://doi.org/10.1038/nmat4170>.

- [24] Pumera M. Graphene-based nanomaterials for energy storage. *Energy Environ Sci* 2011;4:668–74. <https://doi.org/10.1039/C0EE00295J>.
- [25] Singh S, Bhatnagar A, Shukla V, Vishwakarma AK, Soni PK, Verma SK, et al. Ternary transition metal alloy FeCoNi nanoparticles on graphene as new catalyst for hydrogen sorption in MgH₂. *Int J Hydrogen Energy* 2020;45:774–86. <https://doi.org/10.1016/j.ijhydene.2019.10.204>.
- [26] Liu G, Wang Y, Xu C, Qiu F, An C, Li L, et al. Excellent catalytic effects of highly crumpled graphene nanosheets on hydrogenation/dehydrogenation of magnesium hydride. *Nanoscale* 2013;5:1074–81. <https://doi.org/10.1039/c2nr33347c>.
- [27] Huang Y, Xia G, Chen J, Zhang B, Li Q, Yu X. One-step uniform growth of magnesium hydride nanoparticles on graphene. *Prog Nat Sci Mater Int* 2017;27:81–7. <https://doi.org/https://doi.org/10.1016/j.pnsc.2016.12.015>.
- [28] Liu R, Zhao Y, Chu T. Theoretical exploration of MgH₂ and graphene nano-flakes in cyclohexane: proposing a new perspective toward functional hydrogen storage material. *Chem Commun* 2015;51:2429–32. <https://doi.org/10.1039/C4CC09424G>.
- [29] Li W, Huang J, Feng L, Cao L, Feng Y, Wang H, et al. Facile: In situ synthesis of crystalline VOOH-coated VS₂ microflowers with superior sodium storage performance. *J Mater Chem A* 2017;5:20217–27. <https://doi.org/10.1039/c7ta05205g>.
- [30] Fang W, Zhao H, Xie Y, Fang J, Xu J, Chen Z. Facile Hydrothermal Synthesis of VS₂/Graphene Nanocomposites with Superior High-Rate Capability as Lithium-Ion Battery Cathodes. *ACS Appl Mater Interfaces* 2015;7:13044–52. <https://doi.org/10.1021/acsami.5b03124>.
- [31] Ma H, Shen Z, Ben S. Understanding the exfoliation and dispersion of MoS₂ nanosheets in pure water. *J Colloid Interface Sci* 2018;517:204–12. <https://doi.org/10.1016/j.jcis.2017.11.013>.
- [32] Lu X, Utama MIB, Zhang J, Zhao Y, Xiong Q. Layer-by-layer thinning of MoS₂ by thermal annealing. *Nanoscale* 2013;5:8904–8. <https://doi.org/10.1039/C3NR03101B>.

- [33] Chakraborty B, Matte HSSR, Sood AK, Rao CNR. Layer-dependent resonant Raman scattering of a few layer MoS₂. *J Raman Spectrosc* 2013;44:92–6. <https://doi.org/https://doi.org/10.1002/jrs.4147>.
- [34] Hazarika SJ, Mohanta D. Inorganic fullerene-type WS₂ nanoparticles: processing, characterization and its photocatalytic performance on malachite green. *Appl Phys A* 2017;123:381. <https://doi.org/10.1007/s00339-017-0965-7>.
- [35] Berkdemir A, Gutiérrez HR, Botello-Méndez AR, Perea-López N, Elías AL, Chia C-I, et al. Identification of individual and few layers of WS₂ using Raman Spectroscopy. *Sci Rep* 2013;3:1755. <https://doi.org/10.1038/srep01755>.
- [36] Frindt RF. Single Crystals of MoS₂ Several Molecular Layers Thick. *J Appl Phys* 1966;37:1928–9. <https://doi.org/10.1063/1.1708627>.
- [37] Radisavljevic B, Radenovic A, Brivio J, Giacometti V, Kis A. Single-layer MoS₂ transistors. *Nat Nanotechnol* 2011;6:147–50. <https://doi.org/10.1038/nnano.2010.279>.
- [38] Ovchinnikov D, Allain A, Huang Y-S, Dumcenco D, Kis A. Electrical Transport Properties of Single-Layer WS₂. *ACS Nano* 2014;8:8174–81. <https://doi.org/10.1021/nn502362b>.
- [39] Kissinger HE. Reaction Kinetics in Differential Thermal Analysis. *Anal Chem* 1957;29:1702–6. <https://doi.org/10.1021/ac60131a045>.
- [40] Wu Z, Fang J, Liu N, Wu J, Kong L. The Improvement in Hydrogen Storage Performance of MgH₂ Enabled by Multilayer Ti₃C₂. *Micromachines* 2021;12. <https://doi.org/10.3390/mi12101190>.
- [41] Lima EC, Hosseini-Bandegharai A, Moreno-Piraján JC, Anastopoulos I. A critical review of the estimation of the thermodynamic parameters on adsorption equilibria. Wrong use of equilibrium constant in the Van't Hoof equation for calculation of thermodynamic parameters of adsorption. *J Mol Liq* 2019;273:425–34. <https://doi.org/https://doi.org/10.1016/j.molliq.2018.10.048>.
- [42] Chen J, Cao J, Zhou J, Zhang Y, Li M, Wang W, et al. Mechanism of highly enhanced hydrogen storage by two-dimensional 1T' MoS₂. *Phys Chem Chem Phys* 2020;22:430–6. <https://doi.org/10.1039/c9cp04402g>.
- [43] Singh MK, Bhatnagar A, Pandey SK, Mishra PC, Srivastava ON. Experimental

and first principle studies on hydrogen desorption behavior of graphene nanofibre catalyzed MgH₂. *Int J Hydrogen Energy* 2017;42:960–8.
<https://doi.org/10.1016/j.ijhydene.2016.09.210>.